(REFEREED RESEARCH)

# INVESTIGATION OF X-RAY ATTENUATION AND THE FLEX RESISTANCE PROPERTIES OF FABRICS COATED WITH TUNGSTEN AND BARIUM SULPHATE ADDITIVES

# TUNGSTEN VE BARYUM SÜLFAT KATKILI KAPLANMIŞ KUMAŞLARIN X-RAY ZAYIFLATMA VE EĞİLME DAYANIMI ÖZELLİKLERİNİN İNCELENMESİ

**Nebahat ARAL, F. Banu NERGİS, Cevza CANDAN**

*Istanbul Technical University, Department of Textile Engineering, Istanbul, Turkey*

Received: 17.08.2015 Accepted: 25.02. 2016

**ABSTRACT**

In this paper, the x-ray attenuation and the flex resistance properties of lead free, textile based shielding materials were investigated. As an alternative to lead, tungsten and barium sulphate powders were used as radiopaque additives in textile. The cotton fabrics were coated with silicone rubber that contains tungsten and barium sulphate powders in equal weight fractions (60%). X-ray attenuation ratios of samples were measured at 80kV, 100kV, and 150kV tube voltages in accordance with medical protection standards. Besides, the durability of the coatings on textile surface against repetitive folding was observed and the surfaces were examined by SEM and EDS techniques. The results showed that the tungsten additives in silicone rubber coating had better attenuation ratios when compared to the samples coated with barium sulphate-silicone rubber at similar thicknesses. In addition to this, tungsten-silicone rubber coated fabrics showed high flex resistance, where some cracks were observed on barium sulphate-silicone rubber coating.

**Keywords:** X-ray shielding, protective textiles, coated fabric, lead free, flex resistance

**ÖZET**

Bu çalışmada, tekstil bazlı kurşun içermeyen kalkanlama malzemelerinin x-ray atenuasyon ve eğilme dayanımı özellikleri incelenmiştir. Kurşuna alternatif, tungsten ve baryum sülfat tozları radyopak katkı olarak tekstil kaplaması içerisinde kullanılmıştır. Pamuklu kumaşlar ağırlıksal olarak eşit miktarda (%60) tungsten ve baryum sülfat katkı içeren silikon kauçuk ile kaplanmıştır. Numunelerin x-ray atenuasyon oranları medikal korunma standartları göz önünde bulundurularak 80kV, 100kV ve 150kV tüp voltajı seviyelerinde ölçülmüştür. Bunun yanı sıra, tekstil yüzeyi üzerindeki kaplamanın tekrarlı eğilmelere karşı dayanımı gözlemlenmiş ve yüzeyler SEM ve EDS teknikleri kullanılarak değerlendirilmiştir. Sonuçlara göre tungsten katkı içeren silikon kauçuk kaplamalı numuneler baryum sülfat-silikon kauçuk kaplamalılara göre aynı kalınlıkta daha iyi atenuasyon oranlarına sahip olmuştur. Bununla beraber, baryum-silikon kauçuk kaplamalarda eğilme testi sonucunda yüzeyde çatlaklar meydana gelirken, tungsten-silikon kauçuk kaplamalı kumaşlar yüksek eğilme dayanımı göstermiştir.

**Anahtar Kelimeler:** X-ray kalkanlama, koruyucu tekstiller, kaplama kumaş, kurşunsuz, eğilme dayanımı

**Corresponding Author:** Nebahat ARAL e-mail: nebahataral@yahoo.com

## 1. INTRODUCTION

The shielding equipment for the operating personal and patient is mainly based on lead materials, which must be worn to be protected from the harmful effects of scattering x-ray radiation during radiological operations [1]. On the other hand, the high level toxicity of lead is a major problem of lead based shielding equipment, which motives the recent studies to focus on designing non-lead compositions [2-4]. Furthermore, the formation of cracks and holes on lead sheets in shielding equipment (e.g. apron) is another concern due to bending and incorrect hanging after use, which decreases the protection level dramatically and makes the equipment unusable [5,6].The recent studies about lead free shielding materials have focused on developing processes that incorporate radiopaque powders into polymer sheets with sufficient particle content for effective shielding [4,7,8].

The conventional textiles and coating materials consist of low atomic numbered elements (C, H, O etc.) which do not have significant attenuation against x-rays. On the other hand, tungsten and barium sulphate are proven shielding materials that are used in various fields for x-ray attenuation [9,10]. Heavy metal elements (high Z materials) such as tungsten and composites of this material have been traditionally used for protection against x-rays or γ rays because of its higher mass density [11, 12]. Low toxic character makes tungsten a convenient candidate for lead free shielding materials [2, 13]. In studies [12] and [14], tungsten was used in polymer compositions to enhance the attenuation properties of the materials which can be used in shielding of ionizing radiation. In some studies, barium sulphate ($BaSO_4$) was used for radiation protection [8, 10], which is also an environmentally friendly radiopaque material. In [8], medical radiation shielding sheet with the thickness of 1.6 mm was manufactured by using $BaSO_4$ and a combination of tourmaline, tungsten, silicon and rubber polymer, with the aim of composing lead free shielding aprons to reduce the harmfulness. On the other hand, the physical properties of the materials, which were proposed to be used as a wearable structure, were not presented in this study.

In the light of the literature, studies on the flex resistance of polymer composition to folding during usage as protective clothing are limited. Therefore, the aim of this study has been to develop a flexible and lead free coated textile which can be utilized as protective clothing against x-rays, by using relevant conventional textile technologies. Hence, tungsten and barium sulphate powders were used for coating the cotton fabric surface to design a non-lead, flex resistant wearable shield. Moreover; silicone rubber, which is also utilized in various medical textile coatings, was preferred as coating material with the advantage of high adhesion to cotton and very good flexibility [15]. According to medical equipment standards x-ray attenuation properties of coated fabrics were evaluated at certain energy levels. In addition to that, the flex resistance of textile based samples was investigated and the results were discussed by considering the imaging techniques.

## 2. MATERIALS AND METHODS

### 2.1. Sample preparation

Tungsten (W) powder (Sigma Aldrich – average particle size 12 μm) with 19.3 g/cm$^3$ density and barium sulphate ($BaSO_4$) powder (Baser Mining Company – particle size less than 5 μm) with 4.5 g/cm$^3$ density were utilized as powder materials whereas silicone rubber (Terra Silicone Silastosil LSR36, density: 1.11g/cm$^3$ after curing) was chosen as the coating material due to its high viscosity (64 Pa.s) in order to hold powders with high density in dispersed form. As the base for the coating, 100% cotton, plain weave fabric was used with 0.29 mm of thickness and 110 g/m$^2$ of fabric weight. The warp and weft density values of the fabric are 29 and 31 thread/cm, respectively.

The coating compound was prepared by mixing powder additives (tungsten or barium sulphate in powder form) and the silicone rubber with 60% additive weight ratio for 1 hour by Heidolph 2041 mechanical mixer. The compound was degassed by vacuuming for 30 minutes before the coating process to avoid air bubbling in silicone rubber. RGK 40 laboratory type knife coating machine from Atac Machine Corporation was used for the fabric coating process with knife over roll position technique. The curing condition of the silicone rubber compound was determined as 15 minutes at the temperature of 110°C. The properties of the samples are given in Table 1. The average values of weight and thickness of the base fabric and the coated fabric are also given in Table 2.

**Table 1.** The properties of the SR-Tungsten and SR-$BaSO_4$ samples

| Sample | Coating material | Powder additive | Additive density (g/cm$^3$)[16] | Additive weight ratio (%) | Additive volume ratio (%) |
|---|---|---|---|---|---|
| **SR-Tungsten** | Silicone Rubber | Tungsten | 19.3 | 60 | 7.94 |
| **SR-$BaSO_4$** | Silicone Rubber | Barium Sulphate | 4.5 | 60 | 27.23 |

**Table 2.** The average weights and thicknesses for SR-Tungsten and SR-$BaSO_4$ samples

| | SR-Tungsten | SR-$BaSO_4$ |
|---|---|---|
| Base fabric thickness (mm) | 0.290 | 0.290 |
| Total thickness (mm) | 0.410 | 0.405 |
| Base fabric weight (g/m$^2$) | 110.00 | 110.00 |
| Total weight (g/m$^2$) | 714.95 | 586.59 |

## 2.2. Measurement of X-ray Attenuation

In accordance with the standard IEC 61267: 2005 [17], the radiation attenuation values of the samples were measured at 80kV, 100kV, and 150kV tube voltages at Turkish Atomic Energy Authority, Nuclear Research Center. The distance between the x-ray tube and the detector was set to 100 cm, and the x-ray beam was well collimated according to the size of the sample (9 cm x 9 cm). The fabric samples were placed between the detector and the x-ray source, at a very close position to the detector. The schematic representation of the x-ray attenuation measurement setup is given in Figure 1.

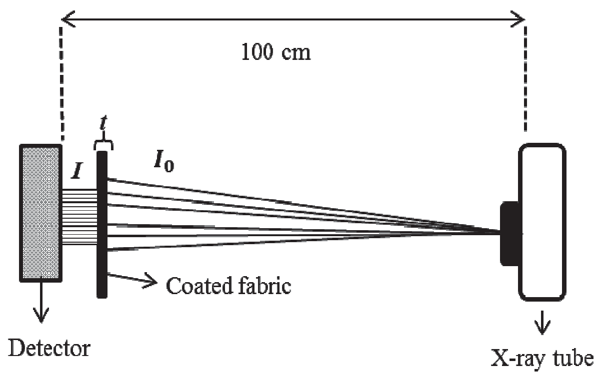


**Figure 1.** The x-ray attenuation measurement setup

X-ray attenuation properties of a material are described by exponential attenuation law. The relation between x-ray and matter is given by Equation 1 [18].

$$I/I_0 = e^{-\mu t} \quad (1)$$

In Equation 1, I is the intensity of the attenuated beam, $I_0$ is the initial intensity, t (cm) is the thickness of the shielding material and μ (1/cm) is the attenuation coefficient of the shielding material [18]. In practical terms, I is the intensity of x-ray radiation after interaction with the shielding material, and I depends on $I_0$, material thickness, and attenuation coefficient. Attenuation coefficient (μ) is a characteristic property of the material which varies with the x-ray energy level.

Radiation attenuation ratios (RAR) of each sample are calculated by Equation 2:

$$RAR\ (\%) = \frac{I_0 - I}{I_0} \quad (2)$$

## 2.3. Measurement of Flex Resistance and Scanning Electron Microscopy (SEM) and Energy Dispersive Spectroscopy (EDS)

The flex resistance measurements of the coated fabrics were done by flexometer method in dry conditions, according to ISO 5402-1:2011[19]. The two edges of the samples with the size of 45 × 70 mm were attached to the clamps of the flexometer device. In each cycle of the device, the samples were subjected to harsh creasing motion, which is focused along the centerline by the moving fold. According to the ISO standard, the samples were observed after each predetermined cycles and the folding process continued until any damage was detected.

The coated sides of the fabric surface were characterized by using an FEI Quanta FEG 200 SEM and METEK EDAX Apollo X for Energy Dispersive Spectroscopy (EDS) analysis. For clear imaging, samples were coated with 5nm of Palladium and Gold (Pd-Au) by using Quorum SC7620 ion sputtering equipment. SEM images were taken at x 15.000 and x 1.000 magnifications.

# 3. RESULTS AND DISCUSSION

In this section, the results of x-ray attenuation and the flex resistance measurements of the samples SR-Tungsten and SR-$BaSO_4$ were presented. The shielding performances of the fabrics were given in terms of radiation attenuation ratios (RAR) which were calculated by Equation (2). The flex performance of the samples was also evaluated which includes a visual examination process. Moreover, the SEM images and EDS graphics were also presented.

## 3.1. X-ray radiation measurements

In Figure 2, the radiation attenuation ratios of SR-Tungsten and SR-$BaSO_4$ are given at three tube voltage levels, namely 80kV, 100kV, and 150kV. As it may be seen from Figure 2, the fabrics having the tungsten powder embedded coating showed higher shielding abilities than the barium sulphate coated fabrics at each energy level. Tungsten element in pure form with its high atomic number (Z=74) and high attenuation coefficient has the ability to attenuate higher incidence of x-rays than barium (Z=56) at current energies [20]. Therefore, at same additive weight ratios (60%) it can be expected that the coating with tungsten powder additives attenuates more radiation than coating with barium sulphate. Moreover, the attenuation ratios of the samples declined under increment of x-ray energy levels due to the higher incident intensities (i.e $I_0$) (Equation 1).

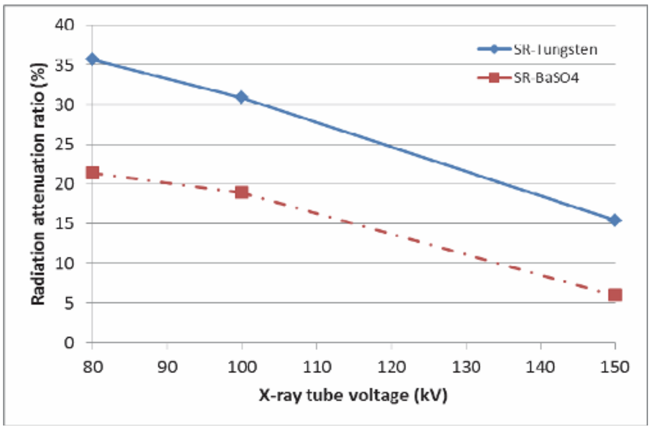


**Figure 2.** Radiation attenuation ratios of the single layer of SR-Tungsten and SR-$BaSO_4$

The results showed that the single layer of the coated fabrics had insufficient protection at the energy levels studied (Figure 2). As Equation 1 suggested, the thickness of a shielding material (i.e. *t*) has an important role in radiation shielding where higher thicknesses result in lower $I/I_0$ values. In order to enhance the shielding ratios, the total thickness of the samples were increased by composing layered structures in a sandwich form. SR-Tungsten and SR-$BaSO_4$ samples from one to five layers were tested under 100kV energy level.

As can be seen in Figure 3 and Table 3, the radiation attenuation ratio of SR-Tungsten sample composed of five layers reached 76.1%, whereas it was 60.5% for the equivalent SR-$BaSO_4$ sample. Moreover, it may also be seen that higher attenuation ratios were observed (Table 3) for thicker structure as expected by considering the radiation attenuation law (Equation 1).

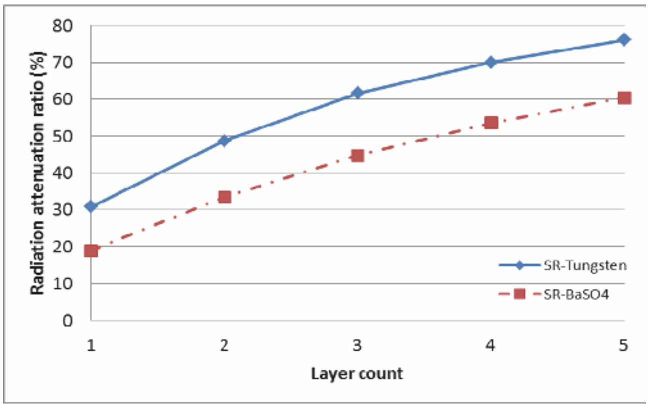


**Figure 3.** Radiation attenuation ratios of the layered structures at 100kV tube voltage

According to the data (Table 3), the layered samples coated with the tungsten powder additives had better shielding abilities when compared to the ones composed of the barium sulphate powder at similar thicknesses. Therefore, it can be mentioned that barium sulphate embedded samples are needed to be thicker to have the same radiation attenuation ratios (RAR) with tungsten embedded samples, which results in to higher weights (Table 3).

According to the radiation protection standards, the personal protective materials against x-rays in medical applications should have the attenuation performance of 90% or higher which means a protective equivalent of not less than 0.25 mm lead for x-rays up to 100 kV [21]. The samples with the attenuation ratio of 76.1% (5 layered SR-Tungsten) and 60.5% (5 layered SR-$BaSO_4$) have the lead equivalent thicknesses of 0.123mmPb and 0.03mmPb, respectively. However, these values should be improved by increasing the total thickness and the additive powder ratios in coating to satisfy the required lead equivalence of 0.25mmPb and 0.50mmPb.

### 3.2. Flex Resistance, SEM, and EDS

The durability of coating on fabric surface is critical to obtain required protection in practical terms since the radiation penetrates easily through cracks. Therefore, the silicone rubber coated samples that include tungsten and barium sulphate powders were evaluated by flexometer test method in dry conditions.

As may be seen from Table 4, up to 50.000 cycles no damage was detected on both SR-Tungsten and SR-$BaSO_4$ samples. Later on, the coated surfaces of each sample were observed when the cycle count approached 75.000. At this stage, no defect was detected on the surface of SR-Tungsten samples, on the other hand, some cracks were detected on SR-$BaSO_4$ samples as can be seen in Figure 4-b and c. The flex resistance test of SR-Tungsten samples proceeded until the maximum cycle counts (250.000) were mentioned in the ISO 5402-1:2011 standard. After the completion of 250.000 cycles, no significant signs of cracking, delamination, and discoloration were observed on silicone rubber-tungsten coated fabrics (Fig. 3-a).

In the light of the literature, it is known that the particle loading of additives affects the mechanical properties of polymer composites [22]. In this study, the weight ratio of the additives in both SR-Tungsten and SR-$BaSO_4$ samples is 60%. However, as may be seen from the Table 1, the barium sulphate volume ratio in the coating was 27.3% whilst the tungsten volume ratio was found out to be only 7.4%, due to the difference between their densities which are 4.5 g/cm$^3$ (barium sulphate) and 19.3 g/cm$^3$ (tungsten). The results (Table 4) indicate that the SR-Tungsten samples with lower powder volume ratio seem to reach a satisfactory flexibility level. On the other hand, barium sulphate embedded silicone rubber coating with higher particle loading, showed poor durability against repetitive folding which can be explained that the flexible character of the matrix was weakened by high powder volume ratio (Table 1). Consequently, the results signify that the amount of the additives in coating material should be limited by considering the mechanical performance of the fabrics.

**Table 3.** The properties of SR-Tungsten and SR-$BaSO_4$ layered structure

| | **SR-Tungsten** | | | **SR-$BaSO_4$** | | |
|---|---|---|---|---|---|---|
| Layer counts | RAR (%) | Total thickness (mm) | Total weight (g/m$^2$) | RAR (%) | Total thickness (mm) | Total weight (g/m$^2$) |
| 1 | 30.9 | 0.410 | 714.95 | 18.9 | 0.405 | 586.59 |
| 2 | 48.7 | 0.820 | 1430.00 | 33.4 | 0.810 | 1173.18 |
| 3 | 61.6 | 1.230 | 2144.85 | 44.7 | 1.215 | 1759.77 |
| 4 | 70.0 | 1.640 | 2859.80 | 53.5 | 1.620 | 2346.36 |
| 5 | **76.1** | 2.050 | **3574.75** | **60.5** | 2.025 | **2932.95** |

**Table 4.** The results of flex resistance test

| | Flex cycle counts | | | | | | |
|---|---|---|---|---|---|---|---|
| | **25.000** | **50.000** | **75.000** | **100.000** | **150.000** | **200.000** | **250.000** |
| **SR-Tungsten** | No damage | No damage | No damage | No damage | No damage | No damage | No damage |
| **SR-$BaSO_4$** | No damage | No damage | Cracks | - | - | - | - |

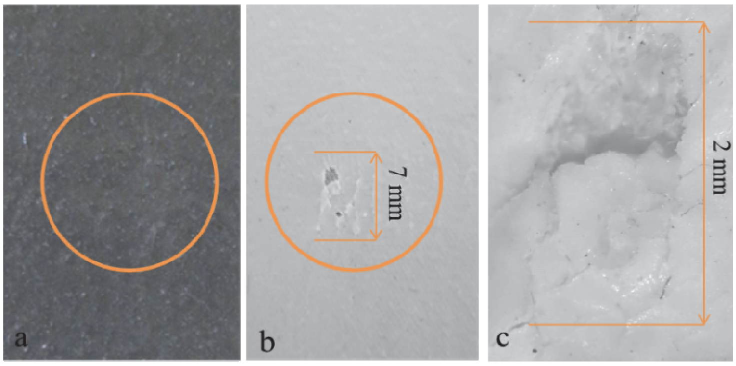


**Figure 4.** The images of SR-Tungsten (a) after 250.000 cycles and SR-$BaSO_4$ (b) after 75.000 cycles of flex, the zoomed image of damaged area on SR-$BaSO_4$ (c).

The elemental distribution graphics and the images also corroborated this significant difference between the particle volume ratios of the samples which is thought to be effective on flex resistance. The SEM micrographs of SR-Tungsten and SR-$BaSO_4$ samples at x 15.000 and x1000 magnification were shown in Figure 5 and 6. As it can be evaluated visually, at the same weight fraction (60%), there was a notable difference between the powder volume ratios of SR-Tungsten and SR-$BaSO_4$ samples.

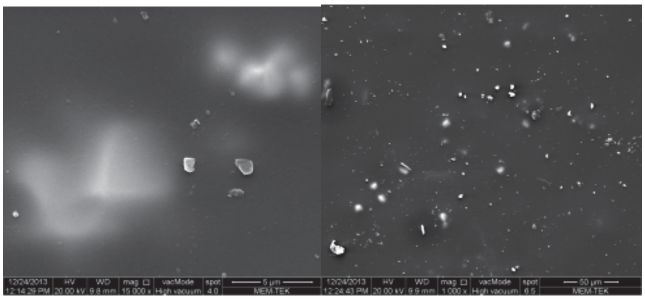

**Figure 5.** SEM micrographs of SR-Tungsten sample coated surface at x15.000 and x1000 magnification

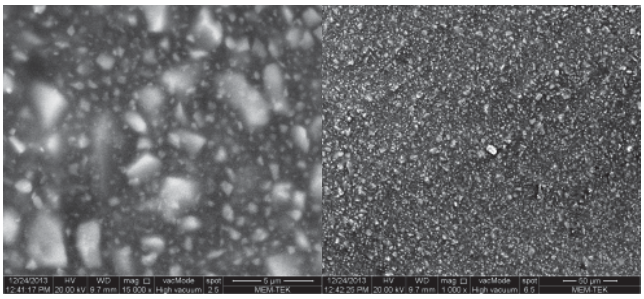

**Figure 6.** SEM micrographs of SR-$BaSO_4$ sample coated surface at x15.000 and x1000 magnification

Besides, the EDS elemental composition graphics of SR-Tungsten and SR-$BaSO_4$ samples were presented in Figure 6. As it may be seen from the graphs, the barium and sulphur values are comparatively higher than the tungsten amount, which indicate that the volume fraction differences of additives in the SR-Tungsten and SR-$BaSO_4$ samples.

In summary, SR-Tungsten samples with higher radiation attenuation ratios with excellent flex resistant reveal that tungsten additives are more convenient than barium sulphate additives in textile coating, when the protection level and durability against folding are taken into consideration. These results are coherent with literature which states that lower volume ratios of tungsten in polymer composites are required to obtain the same level of radiation attenuation of barium sulphate composites while still maintaining good physical and mechanical properties [9].

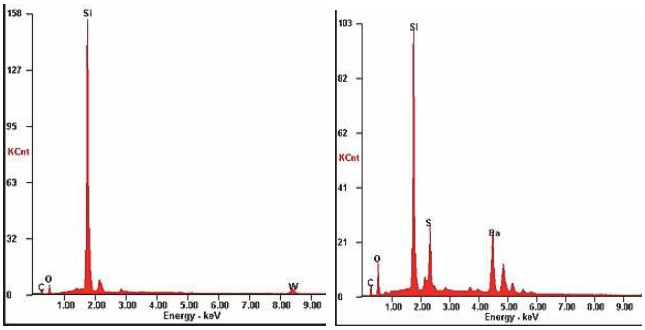


**Figure 7.** EDS elemental composition graphs of SR-Tungsten (left) and SR-$BaSO_4$ (right)

## CONCLUSIONS

In conclusion, the use of tungsten and barium sulphate powder additives in fabric coating can be suggested as a potential method for the design of lead-free protective clothing against X-ray shielding in medical applications.

The tungsten additives at 7.4% volume fraction in silicone rubber coating had a significant effect on shielding with very good flex resistance. In addition to this, the fabrics coated with barium sulphate-silicone rubber blend reached remarkable x-ray attenuation ratios. However, it should be noted that the coatings should be improved for further studies to make them have better shielding ratios (i.e. over 90%). The radiation shielding performance of the coating may be improved by increasing the volume ratio of the additives in the coating where the silicone rubber polymer has nearly no effect on attenuation. On the other hand, the low flex resistance properties of SR-$BaSO_4$ samples with high additive volume ratio, indicates a tradeoff between radiation attenuation and mechanical properties.

In future studies, the effect of increasing volume ratios on attenuation ratios should be analyzed to optimize the shielding ability and the durability of the fabrics.

**ACKNOWLEDGMENTS**

This work was supported by TUBITAK (The Scientific & Technological Research Council of Turkey) under the grant number 112M453 and Istanbul Technical University, BAP project under the grant number 37057. The authors wish to express their appreciation to Lale SEN (Poliser PU Synthesis R&D Manager) and Flokser Textile for their help in carrying out the flex resistance test.

**REFERENCES**


1. Schueler, B.A., 2010, "Operator Shielding: How and Why?", *Tech Vasc Interventional Rad,* 13, 167-171.
2. Martinez, T.P., Cournoyer M.E., 2001, "Lead substitution and elimination study", *Journal of Radioanalytical and Nuclear Chemistry*, Vol. 249, No. 2, 397–402.
3. Scuderi, G.J. et al., 2006, "Evaluation of non–lead based protective radiological material in spinal surgery", *The Spine Journal,* 6, 577–582.
4. Zuguchi, M. et al., 2008, "Usefulness of non-lead aprons in radiation protection for physicians performing interventional procedures" *Rad Prot Dosi*, Vol. 131, No. 4, pp. 531–534.
5. Oyar, O. et al., 2011, "How protective are the lead aprons we use against ionizing radiation?" *Diagn Interv Radiol* 18(2), 147-52.
6. Duran, E.B., Philips B., 2003 (updated 2014), "Rejection criteria for defects in lead apparel used for radiation protection of X-ray workers." *Radiation Protection Services*, British Columbia Centre for Disease Control.
7. Nambiar, S., Osei, E. K., Yeow, J.T., 2013, "Polymer nanocomposite□based shielding against diagnostic x□rays", Journal of Applied Polymer Science, 127(6), 4939-4946.
8. Kim, S.C. et al., 2012, "Medical radiation shielding effect by composition of barium compounds", *Annals of Nuclear Energy*, 47 1–5.
9. Sastri, V.R., 2010, Chapter 5. "Polymer additives used to enhance material properties for medical device applications", *Plastics in Medical Devices*, 55-72.
10. El-Sarraf, M.A. et al., 2013, "Insulating epoxy/barite and polyester/barite composites for radiation attenuation", *App Rad and Iso*, 7918–24.
11. Kobayashi, S. et al., 1997, "Tungsten alloys as radiation protection materials", *Nuc Inst and Met in Physics Res,* A 390, 426-430.
12. Yue, K. et al., 2009, "A new lead-free radiation shielding material for radiotheraphy radiation protection dosimetry", Vol. 133, No. 4, pp. 256–260.
13. Agency for Toxic Substances and Disease Registry, Summary Data For 2015 Priority List of Hazardous Substance. http://www.atsdr.cdc.gov/spl/
14. McCaffrey, J. P., et al., 2007, Radiation attenuation by lead and nonlead materials used in radiation shielding garments. *Medical physics*, 34.2: 530-537.
15. Morton, M., 1999, Chapter 13, Silicone Rubber, Rubber Technology, Springer Science, Business Media Dordrecht, J. C. 375-409.
16. David R., Lide, 1993, CRC Handbook of Chemistry and Physics, 1993, 73rd edition, CRC Press, Boca Raton p.706,734,746.
17. IEC 61267: 2005. Medical diagnostic X-ray equipment - Radiation conditions for use in the determination of characteristics.
18. Hubbell, JH. et al., 1995, "Tables of X-ray mass attenuation coefficients and mass energy-absorption coefficients 1 keV to 20 MeV for elements z = 1 to 92 and 6048 additional substances of dosimetric interest." Technical Report NISTIR-5632.
19. ISO 5402-1:2011 Leather, Determination of flex resistance, Part 1: Flexometer method
20. Berger, M. et al., 2010, XCOM: photon cross sections database at: http://www.nist.gov/pml/data/xcom/index.cfm.
21. Finnerty, M., Brennan, P.C., 2005, "Protective aprons in imaging departments: manufacturer stated lead equivalence values require validation", *Eur Radiol*, 15, 1477–1484.
22. Fu, S.Y. et al., 2008, "Effects of particle size, particle/matrix interface adhesion and particle loading on mechanical properties of particulate–polymer composites" Composites: Part B 39, 933–961.